Synthesis, structure and kinetic studies on $[RuCl_2(NCCH_3)_2(cod)]$

JESÚS J. PÉREZ-TORRENTE*†, CARMEN CUNCHILLOS†, DANIEL GÓMEZ-BAUTISTA†, M. VICTORIA JIMÉNEZ†, RICARDO CASTARLENAS†, FERNANDO J. LAHOZ† and LUIS A. ORO*§

† Departamento de Química Inorgánica, Instituto de Síntesis Química y Catálisis Homogénea-ISQCH (Universidad de Zaragoza-CSIC), C/ Pedro Cerbuna, 12. 50009-Zaragoza, Spain.

§ King Fahd University of Petroleum and Minerals, KFUPM Visiting Professor, Dhahran 31261, Saudi Arabia.

(Received ## March 2012; in final form ### 2012)

The labile compound $[RuCl_2(NCCH_3)_2(cod)]$, an alternative starting material to $[RuCl_2(cod)]_n$ for the preparation of ruthenium(II) complexes, has been prepared from the polymer compound and isolated in yields up to 87% using a new work up procedure. The compound has been obtained as a yellow solid without water of crystallization. Complexes $[RuCl_2(NCR)_2(cod)]$ spontaneously transform into the dimer compounds $[Ru_2Cl(\mu\text{-}Cl)_3(cod)_2(NCR)]$ (R = Me, Ph). ^1H NMR kinetic experiments for these transformations evidenced a first-order type kinetic. $[RuCl_2(NCPh)_2(cod)]$ dimerizes slower than $[RuCl_2(NCCH_3)_2(cod)]$ by a factor of ten. The following activation parameters, $\Delta H^{\#} = 114 \pm 3$ kJmol^{-1} and $\Delta S^{\#} = 66 \pm 9$ JK^{-1}mol^{-1} for R = CH_3CN ($\Delta G^{\#} = 94 \pm 5$ kJmol^{-1}, 298.15 K) and $\Delta H^{\#} = 122 \pm 2$ kJmol^{-1} and $\Delta S^{\#} = 75 \pm 6$ JK^{-1}mol^{-1} for R = Ph ($\Delta G^{\#} = 100 \pm 4$ kJmol^{-1}, 298.15 K), have been calculated from the first-order rate constants in the temperature range 294–323 K. The kinetic parameters are in agreement with a two-step mechanism with the dissociation of acetonitrile as the rate-determining step. The molecular structure of compounds $[Ru_2Cl(\mu\text{-}Cl)_3(cod)_2(NCR)]$ (R = Me, Ph) have been determined by X-ray diffraction.

Keywords: Ruthenium; Dimerzation; Kinetics

*Corresponding author. Email: perez@unizar.es; oro@unizar.es

1. Introduction

The polymer compound $[RuCl_2(cod)]_n$ is a useful synthetic precursor that has been widely used as an entry route into ruthenium chemistry [1]. The easy cleavage of the chloro-bridges by neutral ligands, the metathesis reaction with anionic ligands or the replacement of the strongly bonded 1,5-cyclooctadiene ligand, has led to the preparation of a range of ruthenium (II) complexes [2–5]. In general, the syntheses using $[RuCl_2(cod)]_n$ need harsh conditions and long reaction times due to its low solubility. Moreover, a filtration step is generally required to remove the unreacted ruthenium polymer what very often results in moderate yields. In contrast, less attention has been paid to the soluble compound $[RuCl_2(NCCH_3)_2(cod)]$ despite its potential as an equivalent precursor for ruthenium chemistry due to the lability of the acetonitrile ligands [6–11]. In fact, only a handful of compounds have been synthesized from this mononuclear ruthenium (II) complex with the hydridotris(pyrazolyl)borate compound [RuTpCl(cod)] [12], a platform for the synthesis of a range of organometallic compounds [13, 14], as the most notable example. Interestingly, compound $[RuCl_2(NCCH_3)_2(cod)]$ has been recently applied to the synthesis of ruthenium complexes with biological properties and biomedical applications [15–21].

In our opinion, the relatively low yield attained in its preparation and the variable water content of the isolated product are major factors that have discouraged the application of $[RuCl_2(NCCH_3)_2(cod)]$ in synthesis. We have found that this compound dimerizes in solution at room temperature. In fact, the dinuclear compound $[Ru_2Cl(\mu\text{-}Cl)_3(cod)_2(NCCH_3)]$ was observed in the NMR of $[RuCl_2(NCCH_3)_2(cod)]$ when the spectrum is recorded a few minutes later after its dissolution. We report herein a reliable work up for the synthesis of $[RuCl_2(NCCH_3)_2(cod)]$ that leads to isolated yields over 85 % without water of crystallization. In addition, the kinetic of the dimerization of $[RuCl_2(NCR)_2(cod)]$ (R = Me, Ph) complexes has been studied by NMR.

2. Experimental

2.1 *General methods*

All manipulations were performed under a dry argon atmosphere using Schlenk and cannula techniques. Acetonitrile was distilled over CaH_2. Other solvents were obtained from a Solvent Purification System (Innovative Technologies). Standard literature procedures were used to prepare the compounds $[RuCl_2(cod)]_n$ and $[RuCl_2(NCPh)_2(cod)]$ [22]. ^{1}H NMR spectra were recorded on a Bruker Avance 500 operating at 500.13 MHz. Chemical shifts are reported in parts per million and referenced to $SiMe_4$ using the signal of the deuterated solvent. Elemental C, H and N analysis were performed in a Perkin-Elmer 2400 CHNS/O microanalyzer.

2.2 *Synthesis of $[RuCl_2(NCCH_3)_2(cod)]$ (1)*

A 100 mL Schlenk tube was charged with $[RuCl_2(cod)]_n$ (1.00 g, 3.57 mmol), acetonitrile (60 mL) and 1,5-cyclooctadiene (1.0 mL). The suspension was refluxed for 12 h and then filtered while hot through a celite pad to give an orange solution that was brought to dryness under vacuum. The orange-yellow residue was stirred with methanol (3 mL) for 10 min and then diethyl ether (9 mL) was added. The suspension was further stirred for 10 min and then, allowed for settle down and filtered. The washing procedure to remove the soluble compound $[RuCl_2(NCCH_3)_4]$ was repeated three more times. The pale-yellow solid was washed with diethyl ether (3x3 mL) and dried under vacuum overnight. Yield: 87% (1.13 g). Anal. Calcd. for $C_{12}Cl_2H_{18}N_2Ru$ (%): C, 39.79; H, 5.01; N, 7.73. Found: C, 39.68; H, 5.68; N, 7.78. ^{1}H NMR ($CDCl_3$): δ = 4.31 (m, 4H, =CH cod), 2.63 (s, 6H, $NCCH_3$), 2.45 (m, 4H, $>CH_2$ cod), 2.06 (m, 4H, $>CH_2$ cod).

2.3 *Kinetic measurements*

The rate of dimerization of **1** and **3** was measured by ^{1}H NMR spectroscopy. A 5 mm NMR tube containing a $CDCl_3$ solution of $[RuCl_2(NCR)_2(cod)]$ (0.030 M) and methoxybenzene (1.2

mL) was introduced into the NMR probe preheated to the desired temperature (294-323 K). After allowing for thermal equilibration and experiment setup, periodic NMR spectra (typically each 10 min) with identical acquisition parameters were recorded over several hours. Disappearance of complexes $[RuCl_2(NCR)_2(cod)]$ was monitored by ^1H NMR (500.13 MHz) spectroscopy by integrating the resonances of the =CH protons of the cod ligand (4.31 ppm for **1** and 4.42 ppm for **3**) compared to the internal standard methoxybenzene using automatic integration software. The observed rate constants were obtained from linear least square regression analysis. The activation parameters, $\Delta H^{\#}$ and $\Delta S^{\#}$, were calculated from a linear least squares fit of $\ln(k/T)$ *vs.* 1/T (Eyring equation) [23].

2.4 *Crystal Structure Determination*

Single crystals for the X-ray diffraction study of $[Ru_2Cl(\mu\text{-}Cl)_3(cod)_2(NCCH_3)]$ (**2**) and $[Ru_2Cl(\mu\text{-}Cl)_3(cod)_2(NCPh)]$ (**4**) were grown by slow diffusion of diethylether into dichloromethane solutions of the complexes. Intensity data for both structures were collected at low temperature (100(2) K) on a Bruker SMART APEX CCD area diffractometer, using graphite-monochromated Mo Kα radiation (λ = 0.71073 Å). Data were processed using SAINT [24] and corrected for absorption using a multiscan method applied with SADABS program [25–26]. The structures were solved by direct methods with SHELXS-86 [27] and the refinement, by full-matrix least squares on F^2, was carried out with SHELXL97 [28] with anisotropic displacement parameters for all non-hydrogen atoms. Hydrogen atoms were included in calculated positions and refined as riding atoms. All residual peaks were lower than 1.03 $e^-/Å^3$ and were situated close to ruthenium atoms. Crystallographic and structure refinement data are given in table 1.

Table 1

3. Results and discussion

3.1 *Synthesis of [$RuCl_2(NCCH_3)_2(cod)$]*

The polymer $[RuCl_2(cod)]_n$ was obtained as a brown solid directly from the salt $RuCl_3 \cdot xH_2O$ and cyclooctadiene in refluxing ethanol with excellent yields (91-96%, 0.2 mol scale, equation 1). On the other hand, $[RuCl_2(NCCH_3)_2(cod)]$ (**1**) was prepared by refluxing a suspension of $[RuCl_2(cod)]_n$ in acetonitrile and obtained as orange crystals by crystallization from acetonitrile in moderate yield (38-44%, 5.0 mmol scale, equation 2) [22].

$$RuCl_3 \cdot xH_2O + 2\ cod + CH_3CH_2OH \longrightarrow [RuCl_2(cod)]_n + 2\ HCl + CH_3COH \quad (1)$$

$$[RuCl_2(cod)]_n + 2\ CH_3CN \longrightarrow [RuCl_2(NCCH_3)_2(cod)] \quad (2)$$

The crystalline compound **1** was reported to contain varying amounts of water of crystallization as it was found in the X-ray structure that showed a *trans* disposition of the acetonitrile ligands (*OC-6*-33 isomer) [29, 30]. In addition, we have noticed that **1** spontaneously transforms in solution at room temperature into the dinuclear compound $[Ru_2Cl(\mu\text{-}Cl)_3(cod)_2(NCCH_3)]$ (**2**). Thus, in order to optimize the yield in the synthesis of $[RuCl_2(NCCH_3)_2(cod)]$ (**1**) we have investigated further its preparation and chemical behavior.

We have carried out the synthesis of $[RuCl_2(NCCH_3)_2(cod)]$ (**1**) following the reported experimental conditions [22]. Refluxing a suspension of $[RuCl_2(cod)]_n$ (2.76 mmol) in acetonitrile (28 mL) for 5 h in the presence of cod (1 mL), in order to minimize the formation of $[RuCl_2(NCCH_3)_4]$ [31], gave an orange solution after removing an insoluble material. Concentration of the solution to half of the volume and cooling to 258 K gave orange crystals of $\mathbf{1} \cdot xH_2O$ in ≈ 57% yield (1.57 mmol).

We have investigated both the composition of the resulting solution after isolation of **1** and the unreacted recovered solid. The ^1H NMR ($CDCl_3$) of an aliquot of the solution showed

mainly **1** and a small amount of $[RuCl_2(NCCH_3)_4]$, apart from acetonitrile and 1,5-cyclooctadiene, which suggest to modify the work up procedure to increase the isolated yield. In fact, starting from $[RuCl_2(cod)]_n$ (1.00 g, 3.57 mmol), following the same experimental procedure, compound **1** was isolated in 72% yield (0.937 g, 2.59 mmol) as a yellow-orange solid by crystallization from acetonitrile/diethyl ether. Interestingly, compound **1** was obtained free of crystallization water as it was evidenced in the ^{1}H NMR spectrum in dry CD_2Cl_2. However, the 500 MHz ^{1}H NMR spectrum also showed the presence of complex $[RuCl_2(NCCH_3)_4]$ (≈ 5%). This by-product is only observable in the 500 MHz ^{1}H NMR spectra as a sharp singlet at 2.51 ppm. This signal is overlapped with the broad resonance at 2.45 ppm corresponding to $>CH_2$ protons of the cod ligand of **1** in the 300 MHz spectrum. On the other hand, the recovered solid (0.247 g) was shown to contain unreacted starting material and, in fact, it was possible to obtain a second crop of **1** (0.129 g, 0.356 mmol) by reacting this solid again with CH_3CN under the same conditions giving a combined yield of 82%.

In order to improve the conversion of $[RuCl_2(cod)]_n$ to $[RuCl_2(NCCH_3)_2(cod)]$ (**1**) we have undertaken the synthesis under more diluted conditions (1.00 g, 3.57 mmol, in 60 mL of CH_3CN) increasing the reaction time (12 h). The crude compound was purified by washing several times with methanol/diethyl ether following the procedure described in the experimental section. This optimized synthesis allows the isolation of anhydrous **1** in 87% yield (1.13 g, 3.12 mmol), free of $[RuCl_2(NCCH_3)_4]$, minimizing the amount of unreacted solid (see Supplementary materials).

3.2. *Kinetic study and mechanism for the dimerization of $[RuCl_2(NCR)_2(cod)]$ (R = Me, Ph)*

The acetonitrile ligands in $[RuCl_2(NCCH_3)_2(cod)]$ (**1**) are labile. The ^{1}H NMR of **1** in acetonitrile-d^3 at room temperature showed a resonance at 1.96 ppm corresponding to free acetonitrile, which steadily increases with time with concomitant decrease of the resonance at 2.60 ppm of the acetonitrile ligands in **1**, due to acetonitrile exchange. In the same way, the

^{1}H NMR of **1** in DMSO-d^6 evidenced the formation of [$RuCl_2$(DMSO-d^6)$_2$(cod)] (5.50 ppm, 4H, =CH; 2.50, 2.29, 4H each, >CH_2) and free acetonitrile (2.07 ppm).

In addition, **1** spontaneously dimerizes in solution to give the dinuclear compound [$Ru_2Cl(\mu\text{-}Cl)_3(cod)_2(NCCH_3)$] (**2**). The ^{1}H NMR of a solution of **1** in $CDCl_3$ (500 MHz) showed in a few minutes four new resonances at 4.69, 4.53, 4.46 and 4.26 ppm corresponding to the =CH of the cod ligands of **2**. In addition, this spectrum showed two new resonances in the acetonitrile region at 2.67 and 2.01 ppm, that correspond to **2** and free CH_3CN, respectively. The dimerization of **1** also gives a second species (<10%), probably an asymmetric isomer of the dinuclear compound. In the same way, the related benzonitrile complex [$RuCl_2(NCPh)_2(cod)$] (**3**) slowly transforms into the dinuclear compound [$Ru_2Cl(\mu\text{-}Cl)_3(cod)_2(NCPh)$] (**4**). The formation of the dimeric species is a consequence of the lability of the nitrile ligands and the stability of triple halide-bridging ruthenium compounds (figure 1) [32–35].

Figure 1

In order to obtain relevant information for these transformations, the kinetic of the conversion of [$RuCl_2(NCR)_2(cod)$] (R = Me, **1**; Ph, **3**) into [$Ru_2Cl(\mu\text{-}Cl)_3(cod)_2(NCR)$] (R = Me, **2**; Ph, **4**) has been studied by NMR spectroscopy in $CDCl_3$. Disappearance of **1** and **3** was monitored by ^{1}H NMR by integration of the olefinic =CH resonances of the cod ligand at 4.31 and 4.42 ppm, respectively, compared to the internal standard anisole. A typical plot of [**1**] and [**3**] *vs*. t obtained from NMR measurements at $[Ru]_0$ = 0.028 M and 304.15 K is shown in figure 2. As can be seen in the figure the dimerization of the acetonitrile complex **1** is much faster than the benzonitrile complex **3**.

Figure 2

The representation of $\ln([Ru]_0/[Ru])$ *vs*. t for both complexes gave a curve that show a linear fragment which is an indication that the dimerization reaction follows a first-order kinetic up to approximately 65% conversion (figure 3).

Figure 3

The kinetic behavior for the dimerization reaction is compatible with the following mechanism:

$$[RuCl_2(NCR)_2(cod)] \underset{k_{1r}}{\overset{k_{1f}}{\rightleftharpoons}} [RuCl_2(NCR)(cod)] + RCN \quad (3)$$

$$2\,[RuCl_2(NCR)(cod)] \underset{k_{2r}}{\overset{k_{2f}}{\rightleftharpoons}} [Ru_2Cl(\mu\text{-}Cl)_3(cod)_2(NCR)] + RCN \quad (4)$$

The first proposed step is an equilibrium involving the dissociation of an RCN ligand to give the pentacoordinated $[RuCl_2(NCR)(cod)]$ intermediate species. In a second equilibrium step, the assembly of two molecules of this unsaturated species results in the formation of the dimer $[Ru_2Cl(\mu\text{-}Cl)_3(cod)_2(NCR)]$ with extrusion of RCN.

The following rate equation can be written from the first step:

$$-\frac{d[RuCl_2(NCR)_2(cod)]}{dt} = k_{1f}[RuCl_2(NCR)_2(cod)] - k_{1r}[RuCl_2(NCR)(cod)][NCR]$$

Assuming a very small concentration of the intermediate species $[RuCl_2(NCR)(cod)]$ (not observable by NMR) and a low [RCN] at the beginning of the reaction:

$$k_{1f}[RuCl_2(NCR)_2(cod)] > k_{1r}[RuCl_2(NCR)(cod)][NCR]$$

and, under this conditions, the dimerization reaction follows a first-order kinetic [23].

$$-\frac{d[RuCl_2(NCR)_2(cod)]}{dt} = k_{1f}[RuCl_2(NCR)_2(cod)]$$

Thus, the first-order constants k_{obs} (s^{-1}) determined from the slope of the straight section of the $\ln([Ru]_0/[Ru])$ *vs*. t plots correspond to k_{1f}, the rate constant for the RCN dissociation in complexes $[RuCl_2(NCR)_2(cod)]$ [23].

The temperature influence on the reaction rate was investigated in the temperature range 294.15–323.15 K in $CDCl_3$. The first-order observed rate constant, k_{obs} (k_{1f}), determined at different temperatures are shown in table 2. The overall activation parameters were determined using the logarithmic form of the Eyring equation. The kinetic parameters obtained from the Eyring plot (figure 4) were: $\Delta H^{\#} = 114 \pm 3$ kJmol^{-1} and $\Delta S^{\#} = 66 \pm 9$ JK^{-1}mol^{-1} ($\Delta G^{\#} = 94 \pm 5$ kJmol^{-1}, 298.15 K) for **1** (CH_3CN), and $\Delta H^{\#} = 122 \pm 2$ kJmol^{-1} and $\Delta S^{\#} = 75 \pm 6$ JK^{-1}mol^{-1} ($\Delta G^{\#} = 100 \pm 4$ kJmol^{-1}, 298.15 K) for **3** (PhCN). The positive value of entropy term in both cases suggests that the rate-determining step is of a dissociative nature in full agreement with the mechanistic proposal. On the other hand, the higher activation enthalpy for compound **3** suggests that the Ru-NCPh bond is stronger than Ru-$NCCH_3$ bond. In fact, compound **3** was prepared refluxing **1** in PhCN [29], which is full agreement with the kinetic observations.

Table 2 and Figure 4

A kinetic analysis of the proposed dimerization mechanism (equations 3 and 4) using the software Berkeley-Madonna has allowed a rough estimation of the other involved rate constants [36]. The model parameters were estimated by fitting of the [**3**] *vs*. t plot to the experimental data using numerical integration. The obtained values for the dimerization of **3** at 304.15 K were $k_{1f} \approx 0.28$ h^{-1}, $k_{1r} \approx 1240$ Lmol^{-1}h^{-1}, $k_{2f} \approx 5.2 \times 10^5$ h^{-1} and $k_{2r} \approx 2.4 \times 10^{-5}$ Lmol^{-1}h^{-1}. These data support the dissociation equilibrium leading to the unsaturated species $[RuCl_2(NCR)(cod)]$ as the rate-determining step (step 1, $k_{1f} < k_{1r}$), and evidence the fast dimerization of $[RuCl_2(NCR)(cod)]$ (step 2, $k_{2f} >> k_{2r}$).

In principle, the labile character of $[RuCl_2(NCCH_3)_2(cod)]$ (**1**) accounts for its reactivity. However, the fast dimerization into the dinuclear compound $[Ru_2Cl(\mu\text{-}Cl)_3(cod)_2(NCCH_3)]$ (**2**) at the refluxing temperature of most of the standard solvents could be a potential drawback that delimits its synthetic application. Noteworthy, the dimerization process is reversible and the ^1H NMR of **2** in acetonitrile-d^3 shows the clean formation of the mononuclear compound $[RuCl_2(NCCD_3)_2(cod)]$ (**1***). Thus, the trichloro-bridge diruthenium core is easily cleavage even with poor ligands as acetonitrile and compound **2** can be also considered as a precursor of the unsaturated fragment "$RuCl_2(cod)$".

3.4 *Molecular structure of $[Ru_2Cl(\mu\text{-}Cl)_3(cod)_2(NCR)]$ complexes (2 and 4)*

Suitable crystals for X-ray diffraction analysis of the dinuclear complexes $[Ru_2Cl(\mu\text{-}Cl)_3(cod)_2(NCCH_3)]$ (**2**) and $[Ru_2Cl(\mu\text{-}Cl)_3(cod)_2(NCPh)]$ (**4**) were grown from dichloromethane solutions of the complexes coming from the dimerization of **1** and **3**, respectively. The molecular structure of the isostructural complexes **2** and **4** is shown in figure 5. A selection of bond distances and angles is given in table 3. Compound **2** was obtained as a marginal product from reactivity studies on Ru(0) complexes and its crystal structure determined at 295 K [37]. The low temperature crystal structure of **2** (100 K) presented the same space group and very similar unit-cell parameters that the previously determined structure (295 K).

Figure 5 and Table 3

The structure of both complexes consists of a trichloro-bridged diruthenium core with distorted octahedral coordination geometries. Both ruthenium centers are bonded to three bridging chloro ligands and a 1,5-cyclooctadiene molecule, but have different coordination environments as a consequence of the sixth terminal ligand: a chloro in Ru(2), and a nitrile in Ru(1). The structural features are similar to those found in related face-sharing dioctahedral Ru^{II}–Ru^{II} complexes [32–35]. In particular, the Ru–Cl_{term} distances, 2.4095(14) Å in **2** and

2.3821(15) Å in **4**, are shorter than the Ru–Cl_{brid} distances that range from 2.4195(13)-2.4990(14) Å in **2**, and 2.4081(13)-2.4994(14) Å in **4**, with the Ru–Cl_{brid} *trans* to the nitrile ligand the shortest distance. The Ru-Ru distances, 3.2597(13) Å in **2** and 3.2410(9) Å in **4**, lie in the range expected for non-bonded dinuclear Ru(II) complexes of this type (3.28–3.44 Å) [38]. More importantly, the Ru-N bond distance in **4**, 2.020(4) Å, is shorter than in **2**, 2.039(4), which points out to a stronger ruthenium benzonitrile bond that is in full agreement with the kinetic data.

4. Conclusions

The synthesis of the labile compound $[RuCl_2(NCCH_3)_2(cod)]$, an alternative starting material to $[RuCl_2(cod)]_n$ for the preparation of ruthenium(II) complexes, has been investigated. The compound has been obtained free of water of crystallization in yields up to 87% using a new work up procedure. We have found that this compound spontaneously transforms into the dimer $[Ru_2Cl(\mu\text{-}Cl)_3(cod)_2(NCCH_3)]$ at room temperature with the release of acetonitrile. This transformation, that is reversible in the presence of acetonitrile, follows a first order kinetic. The determination of the activation parameters for this process supports a two-step mechanism with the dissociation of acetonitrile as the rate-determining step. Compound $[RuCl_2(NCPh)_2(cod)]$ behaves similarly although the dimerization reaction slows down by a factor of ten.

Supplementary materials

^{1}H NMR (500 MHz) of compound **1**. CCDC-865062 (**2**) and CCDC-865063 (**4**) contain the supplementary crystallographic data. These data can be obtained free of charge from The Cambridge Crystallographic Data Centre via www.ccdc.cam.ac.uk/data_request/cif.

Acknowledgments

Financial support from the Ministerio de Ciencia e Innovación (MICINN/FEDER) of Spain (Project CTQ2010-15221), Diputación General de Aragón (E07) and CONSOLIDER INGENIO-2010, Projects MULTICAT (CSD2009-00050) and Factoría de Cristalización (CSD2006-0015), is gratefully acknowledged.

References

[1] G. Wilkinson (Ed.), *Comprehensive Organometallic Chemistry*, Vol. 4, pp. 748–750, Pergamon Press, Oxford (1982).

[2] B. Jana, A. Ellern, O. Pestovsky, A. Sadow, A Bakac. *Inorg. Chem.,* **50**, 3010 (2011).

[3] G.R. Clark, A. Falshaw, G.J. Gainsford, C. Lensink, A.T. Slade, L. J. Wright. *J. Coord. Chem.*, **63**, 373 (2010).

[4] A.K. Renfrew, A.D. Phillips, E. Tapavicza, R. Scopelliti, U. Rothlisberger, P.J. Dyson. *Organometallics*, **28**, 5061 (2009).

[5] M.E. Morilla, P. Rodriguez, T.R. Belderrain, C. Graiff, A. Tiripicchio, M.C. Nicasio, P.J. Perez. *Inorg. Chem.*, **46**, 9405 (2007).

[6] F. Marchetti, C. Pettinari, R. Pettinari, A. Cerquetella, L.M.D.R.S. Martins, M.F.C. Guedes da Silva, T.F.S. Silva, A.J.L. Pombeiro. *Organometallics*, **30**, 6180 (2011).

[7] M.J. Page, J. Wagler, B.A. Messerle. *Organometallics*, **29**, 3790 (2010).

[8] M.R. Maurya, L.K. Woo. *J. Organomet. Chem.*, **690**, 4978 (2005).

[9] Y. Yamamoto, Y. Nakagai, N. Ohkoshi, K. Itoh. *J. Am. Chem. Soc.*, **123,** 6372 (2001).

[10] T. Hayashida, K. Miyazaki, Y. Yamaguchi, H. Nagashima. *J. Organomet. Chem.*, **634**, 167 (2001).

[11] S. Bennett, S.M. Brown, G. Conole, M. Kessler, S. Rowling, E. Sinn, S. Woodward. *J. Chem. Soc., Dalton Trans*., 367 (1995).

[12] D.C. Wilson, J.H. Nelson. *J. Organomet. Chem.*, **682**, 272 (2003).

[13] E. Becker, S. Pavlik, K. Kirchner. *Adv. Organomet. Chem.*, **56**, 155 (2008).

[14] C. Slugovc, R. Schmid, K. Kirchner. *Coord. Chem. Rev*., **185–186**, 109 (1999).

[15] C. Kasper, H. Alborzinia, S. Can, I. Kitanovic, A. Meyer, Y. Geldmacher, M. Oleszak, I. Ott, S. Wölfl, W.S. Sheldrick. *J. Inorg. Biochem.*, **106**, 126 (2012).

[16] C.L. Donnici, M.H. Araujo, H.S. Oliveira, D.R.M. Moreira, V.R.A. Pereira, M. de Assis Souza, M.C.A. Brelaz de Castro, A.C.L. Leite. *Bioorg. Med. Chem.*, **17**, 5038 (2009).

[17] P.M. Reddy, K. Shanker, R. Rohini, M. Sarangapani, V. Ravinder. *Spectrochimica Acta Part A,* **70**, 1231 (2008).

[18] S. Singh, F. Athar, M.R. Maurya, A. Azam. *Eur. J. Med. Chem.*, **41**, 592 (2006).

[19] L. Zhang, P. Carroll, E. Meggers. *Org. Lett.*, **6**, 521 (2004).

[20] S. Singh, N. Bharti, F. Naqvi, A. Azam. *Eur. J. Med. Chem.*, **39**, 459 (2004).

[21] N.S. Shailendra, N. Bharti, M.T.G. Garza, D.E. Cruz-Vega, J.C. Garza, K. Salem, F. Naqvi, A. Azam. *Bioorg. Med. Chem. Lett.*, **11**, 2675 (2001) and references therein.

[22] M.O. Albers, T.V. Ashworth, H.E. Oosthuizen, E. Singleton. *Inorg. Synth.*, **26**, 68 (1989).

[23] R.G. Wilkins. *Kinetic and Mechanism of Reactions of Transition Metal Complexes*, 2nd Edn, VCH, Weinheim (1991).

[24] SAINT: *Area-Detector Integration Software*, Bruker-AXS, Madison, Viskonsin, USA (1995).

[25] SADABS*, Area Detector Absorption Correction*, Bruker-AXS, Madison, Viskonsin, USA (1996).

[26] R.H. Blessing. *Acta Crystallogr. Sect A*, **51**, 33 (1995).

[27] G.M. Sheldrick. SHELXS86. *J. Mol. Struct.*, **130**, 9 (1985).

[28] G.M. Sheldrick. SHELXL-97, *Program for Crystal Structure Refinement*, University of Göttingen, Germany (1997).

[29] T.V. Ashworth, D.C. Liles, D.J. Robinson, E. Singleton, N.J. Coville, E. Darling, A.J. Markwell. *S. Afr. J. Chem.*, **40**, 183 (1987).

[30] Crystal structure of the acetonitrile solvate: H. Chiririwa, R. Meijboom, S.O. Owalude, U.B. Ekeb, C. Ardernea. *Acta Cryst.* **E67**, m1096 (2011).

[31] R.A. Sánchez-Delgado, M. Navarro, K. Lazardia, R. Atencio, M. Capparellia, F. Vargas, J.A. Urbina, A. Bouillezc, A.F. Noelsc, D. Masid. *Inorg. Chim. Acta*, **275–276**, 528 (1998).

[32] E. Solari, S. Gauthier, R. Scopelliti, K. Severin. *Organometallics*, **28**, 4519 (2009).

[33] C. Albrecht, S. Gauthier, J. Wolf, R. Scopelliti, K. Severin. *Eur. J. Inor. Chem.*, 1003 (2009).

[34] L. Quebatte, R. Scopelliti, K. Severin. *Eur. J. Inor. Chem.*, 231 (2006).

[35] J. Bravo, J. Castro, S. García-Fontán, M.C. Rodríguez-Martínez, P. Rodríguez-Seoane. *Eur. J. Inorg. Chem*., 3028 (2006).

[36] R.I. Macey, G.F. Ester. *Berkeley Madonna v. 8.3*, University of California, Berkeley, California, USA (2001), http://www.berkeleymadonna.com.

[37] H.E. Selnau Jr., J. Mahmoud, L.C. Porter. *Inorg. Chim. Acta*, **224**, 125 (1994).

[38] Y. Borguet, X. Sauvage, G. Zaragoza, A. Demonceau, L. Delaude. *Organometallics*, **30**, 2730 (2011).

Figure Captions

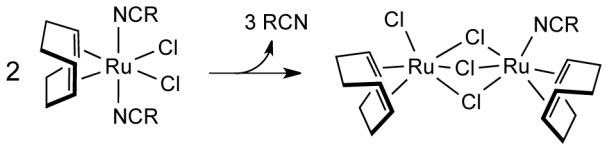

Figure 1. Spontaneous dimerization of $[RuCl_2(NCR)_2(cod)]$ complexes.

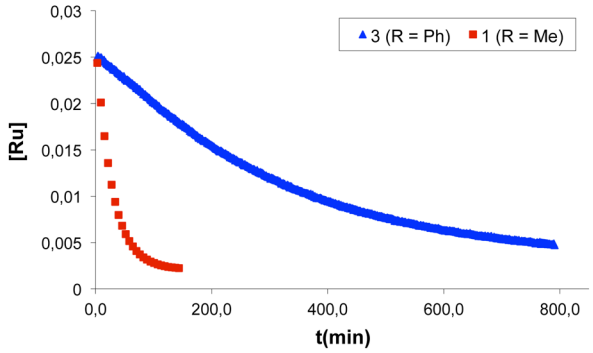

Figure 2. Decay of [**1**] and [**3**] *vs.* time for the conversion of $[RuCl_2(NCR)_2(cod)]$ into $[Ru_2Cl(\mu\text{-}Cl)_3(cod)_2(NCR)]$ (R = Me, Ph) in $CDCl_3$ at 304.15 K determined from ^1H NMR measurements.

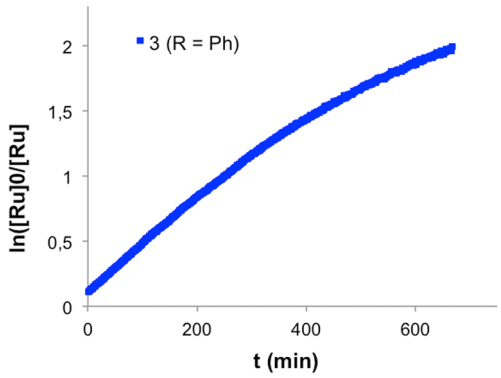

Figure 3. Typical first-order kinetic fit of the data: $\ln([\mathbf{3}]_0/[\mathbf{3}])$ *vs.* time plot for the conversion of **3** into **4** in $CDCl_3$ at 304.15 K.

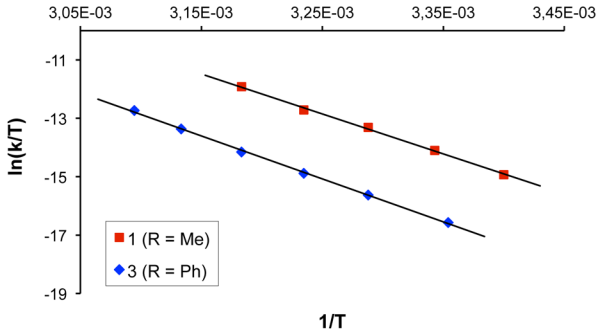

Figure 4. Eyring plot for the dimerization of $[RuCl_2(NCR)_2(cod)]$ into $[Ru_2Cl(\mu\text{-}Cl)_3(cod)_2(NCR)]$ (R = Me, Ph) in $CDCl_3$. The line represents the least squares fit to the data point.

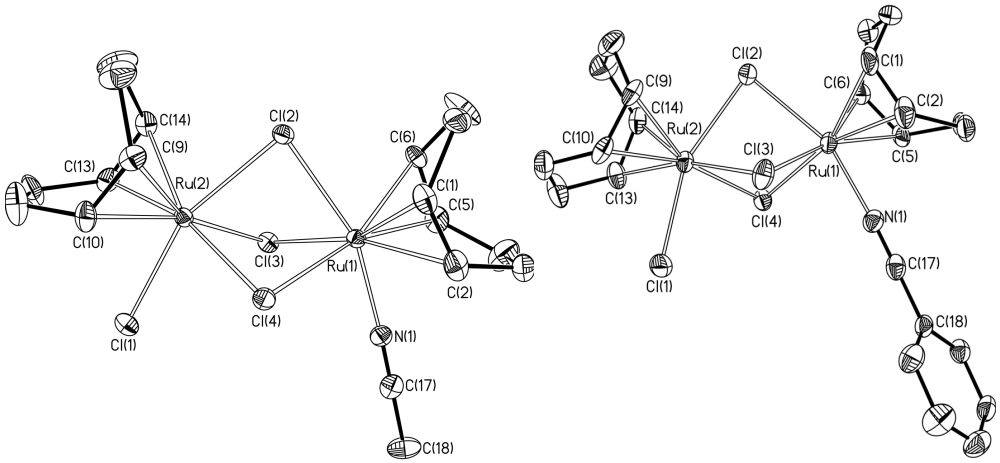

Figure 5. Molecular structures of $[Ru_2Cl(\mu\text{-}Cl)_3(cod)_2(NCCH_3)]$ (**2**) (a) and $[Ru_2Cl(\mu\text{-}Cl)_3(cod)_2(NCPh)]$ (**4**) (b). The hydrogen atoms have been omitted for clarity.

Table 1. Crystal data and structure refinement for **2** and **4**.

Complex	**2**	**4**
Empirical formula	$C_{18}H_{27}Cl_4NRu_2$	$C_{23}H_{29}Cl_4NRu_2$
Formula weight	601.35	663.44
Temperature (K)	100(2)	100(2)
Wavelength (Å)	0.71073	0.71073
Crystal size (mm^3)	0.073 x 0.064 x 0.024	0.106 x 0.096 x
Crystal system	Monoclinic	Monoclinic
Space group	*C*2/c	*C*2/c
a (Å)	21.234(9)	18.244(4)
b (Å)	7.152(3)	16.398(4)
c (Å)	26.760(11)	17.930(4)
β (deg)	92.968(7)	116.346(4)
Volume ($Å^3$)	4058(3)	4807(2)
Z	8	8
Density calculated (g cm^{-3})	1.968	1.834
Absorption coefficient (mm^{-1})	2.018	1.713
θ range for data collection (deg)	1.52 to 28.38	1.76 to 27.05
Reflections collected	13030	15199
Independent reflections	4780 [*R*(int) = 0.0574]	5225 [*R*(int) =
GOF on F^2	1.013	0.975
Final *R* indices [$I > 2\sigma(I)$][a]	$R_1 = 0.0433$	$R_1 = 0.0459$
	$wR^2 = 0.0853$	$wR^2 = 0.0813$
R indices (all data)	$R_1 = 0.0640$	$R_1 = 0.0763$
	$wR^2 = 0.0930$	$wR^2 = 0.0916$
Largest diff. peak and hole ($e \cdot Å^{-3}$)	1.027 and -0.833 $e \cdot Å^{-3}$	0.929 and -0.705

[a] $R_1(F) = \Sigma||F_o| - |F_c|| / \Sigma|F_o|$; $wR_2(F^2) = (\Sigma[w(F_o^2 - F_c^2)^2]/\Sigma[w(F_o^2)^2])^{1/2}$.

Table 2. Temperature dependence of the first-order observed rate constant, k_{obs} (k_{1f}), for RCN dissociation in $[RuCl_2(NCR)_2(cod)]$ complexes ($CDCl_3$).

	1 (R = CH_3)		**3** (R = Ph)	
T/K	k_{1f} (s^{-1})	R^2	k_{1f} (s^{-1})	R^2
294.15	$9.64 \pm 0.05 \times 10^{-5}$	0.996		
299.15	$2.25 \pm 0.02 \times 10^{-4}$	0.996	$1.90 \pm 0.01 \times 10^{-5}$	0.999
304.15	$5.02 \pm 0.04 \times 10^{-4}$	0.998	$4.95 \pm 0.01 \times 10^{-5}$	0.999
309.15	$9.32 \pm 0.1 \times 10^{-3}$	0.996	$1.06 \pm 0.01 \times 10^{-4}$	0.996
314.15	$2.09 \pm 0.07 \times 10^{-3}$	0.994	$2.24 \pm 0.01 \times 10^{-4}$	0.998
319.15			$5.02 \pm 0.03 \times 10^{-4}$	0.999
323.15			$9.54 \pm 0.09 \times 10^{-4}$	0.999

[a] Correlation coefficient

Table 3. Selected Bond Distances (Å) and Angles (°) for **2** and **4.**

	2	**4**
Ru(1)-N(1)	2.039(4)	2.020(4)
Ru(1)-Cl(2)	2.4357(13)	2.4081(13)
Ru(1)-Cl(3)	2.4565(13)	2.4416(14)
Ru(1)-Cl(4)	2.4195(13)	2.4627(14)
Ru(2)-Cl(1)	2.4095(14)	2.3821(15)
Ru(2)-Cl(2)	2.4652(14)	2.4471(14)
Ru(2)-Cl(3)	2.4990(14)	2.4706(14)
Ru(2)-Cl(4)	2.4445(14)	2.4994(14)
N(1)-C(17)	1.130(6)	1.143(6)
C(17)-C(18)	1.456(7)	1.436(7)
Ru(1)-Cl(2)-Ru(2)	83.38(4)	83.75(5)
Ru(1)-Cl(3)-Ru(2)	82.26(5)	82.56(4)
Ru(1)-Cl(4)-Ru(2)	84.16(4)	81.56(4)
C(17)-N(1)-Ru(1)	175.8(4)	174.0(5)
N(1)-C(17)-C(18)	177.2(5)	177.7(6)
N(1)-Ru(1)-Cl(2)	160.02(11)	159.65(12)
N(1)-Ru(1)-Cl(3)	86.68(11)	85.15(13)
N(1)-Ru(1)-Cl(4)	85.55(12)	86.13(12)
Cl(1)-Ru(2)-Cl(2)	158.58(4)	157.62(5)
Cl(1)-Ru(2)-Cl(3)	84.72(5)	84.84(5)
Cl(1)-Ru(2)-Cl(4)	87.39(5)	85.91(5)